

## SATELLITE UV NAVIGATION SYSTEMS

A.A. Cheremisin, L.V. Granitskii, V.A. Bartenev, and I.A. Agapov

*Scientific Research Physico-Technical Institute at the Krasnoyarsk State University  
Krasnoyarsk State Technical University*

*Scientific Production Association "Applied Mathematics," Zheleznogorsk, Krasnoyarsk Krai*

*Received December 3, 1997*

*This paper describes the system for independent spacecraft navigation allowing height determination of star lines above the Earth's surface by measuring star brightness attenuation in the UV wavelength range (200–300 nm) from satellite when observing star set behind the Earth's atmospheric limb. Error of height fixation of star lines is caused by random "weather" variations of atmospheric ozone concentration in the upper atmosphere on one hand and insufficiency of ozone variability model on other hand. Configuration and elements of the promising system allowing simultaneous solution of the problems of independent spacecraft navigation and spacecraft orientation with respect to stars.*

The existing approach for determining the parameters of spacecraft movement in astronavigation is based on measurement of angular distances between known celestial references. The measured angles in this case must be dependent on spacecraft position in the Earth-orbital space and independent of their orientation. Earth, Sun, and stars are taken as celestial references, and devices operating in IR and visible range are used for measuring the angular position of Earth.

Use of an infrared device allows, at best, determination of the vertical error about 3–5 minutes of arc, that results in significant navigation errors. The another approach in development of astronavigation is related with height measurement of star line over the Earth's surface. The line of sight in this case is directed from a spacecraft to a star at the moment of its set or rise. The height can be obtained by measuring the refraction angles.<sup>1,2</sup>

Specialists from the Scientific Research Physico-Technical Institute at the Krasnoyarsk State University in collaboration with specialists from the Krasnoyarsk State University develop the systems for determination of spacecraft navigation parameters based on height estimation of star lines above the Earth's surface from measurements of star brightness in the UV range at star set behind the Earth's atmosphere.

When a star is observed from spacecraft through the Earth's atmosphere, its brightness attenuates depending on the height  $h$  of the line of sight above the Earth's surface. The coefficient of brightness attenuation is

$$\eta(h) = I(h)/I_0,$$

where  $I(h)$  and  $I_0$  are the values of signals from a photoreceiving device when a star is observed through the atmosphere and beyond the atmosphere, respectively;

$$\eta(h) = \frac{\int_{\Lambda} E_{\lambda} F_{\lambda} \eta_{\lambda}(h) d\lambda}{\int_{\Lambda} E_{\lambda} F_{\lambda} d\lambda}, \quad (1)$$

where  $E_{\lambda}$  is the spectral illuminance produced by star;  $F_{\lambda}$  is the relative spectral sensitivity of the photoreceiving device (optical system);  $\eta_{\lambda}(h)$  is the spectral coefficient of transmittance of the Earth's atmosphere;  $\Lambda$  is the operating spectral range of the recording system. We have chosen the UV range of 200–300 nm by the following reasons.

To determine the height of the line of sight from measurements of star brightness attenuation, the height dependence of brightness attenuation must be stable enough. The attenuation coefficient is the function of  $h$  and  $\lambda$ . Variations of spectral transmittance coefficients depend on variations of atmospheric parameters at corresponding altitudes. Star brightness attenuation in the UV range is mainly caused by radiation absorption by atmospheric ozone and observed at altitude of 60–80 km ( $\lambda = 0.25 \mu\text{m}$ ).

In the visible range, star brightness attenuation is observed at altitudes of 20–40 km and caused, first of all, by Rayleigh scattering, then by aerosol scattering, and, to a certain degree, by refraction attenuation. At the same time, influence of variations of atmospheric parameters, such as the aerosol scattering coefficient,<sup>3</sup> on the altitude behavior of the curves of star brightness attenuation and, consequently, on the accuracy of fixation of line of sight is weaker for the UV range as compared to the visible one.

In the visible range, effects of multiple scattering may manifest themselves more markedly. Due to small refraction angles star scintillation at high altitudes observed in the visible range and connected with inhomogeneities of the refraction index (temperature)

in the atmosphere is not observed in the UV range.<sup>4</sup> In the visible range, a significant correction for star line deflection should be taken into account due to large value of refraction angles as compared to the UV range. This results in additional errors connected with the refraction index variations. Besides, the brightness of the sun-illuminated part of the Earth's disk observable from a spacecraft in the UV range is several orders of magnitude smaller than in the visible one. As a consequence, the corresponding illumination background is also lower.<sup>5</sup>

Model computations were performed for curves of star brightness attenuation in the 200–300 nm UV range as functions of systematic (season and latitude) and random ("weather") variations of the atmospheric parameters: altitude dependence of ozone concentration,<sup>6</sup> density of the atmosphere,<sup>7</sup> and aerosol scattering.<sup>3</sup> As seen from computation results, height fixation of experimental curves of star brightness attenuation in the vicinity of 60-km height results in average error not exceeding  $\pm 0.5$  km related to the influence of natural "weather" parameters of the atmosphere. However, the regard for the diurnal behavior of the ozone concentration, comparatively poorly studied at high altitudes, from the data obtained as a result of computations within the framework of photochemical models<sup>8</sup> results in a shift of star brightness attenuation curves of approximately 1.5 km.

With the total linear error of 0.5–2 km, the angular error of fixation of the star line of sight from the geostationary orbits is estimated as 2–10 sec. of arc. The correction for refraction deflection of the star line<sup>9</sup> must also be introduced, because the refraction angle at such altitudes is about several seconds of arc. Computations give small values for variations of the refraction angle due to variability of atmospheric parameters – their relative value is only several percent, and thus they do not contribute significantly into the total error.

The following area of the celestial sphere: declination from  $-3.5^\circ$  to  $+1.5^\circ$ , right ascension from 00:00 to 24:00 (the second equatorial coordinate system), was chosen as the area containing reference stars for the UV device. Selection of reference stars ( $U$  not weaker than  $+6.9^m$ ) was performed from the data of the UV spectrophotometric catalogue TD1 (Ref. 10) and its addendum STD1 obtained at the French satellite TD1.

Selection of the near-equator part of the celestial sphere as an area containing reference stars is related to the fact that altitude distribution of ozone of the near-equator tropical type is most stable. The working area of the above-indicated size in declination was chosen from the wider near-equator area as the one containing the maximum number of bright stars and having their maximum total brightness as compared to other possible zones. Among 57 reference stars 8 stars are varying. If change of the absolute star brightness is not accompanied with relative change of its spectrum, then use of varying stars does not result in error, because the

measured parameter is the relative value of visible change of star brightness.

As follows from Eq. (1), for a specific device having specific spectral sensitivity  $F_\lambda$ , nonzero in the finite area  $\Delta\lambda$ , the altitude attenuation of star brightness is described by a virtually individual curve. The fact that altitude behavior of attenuation curves of signals from stars depends strongly on the curves of spectral sensitivity of a used photoreceiving device (as well as on the spectra of stars themselves) is seen from Fig. 1 presenting the calculated curve (1) of altitude dependence of signal attenuation for one of reference stars (No. 252 from the Catalogue,<sup>10</sup>  $\alpha = 5^h 40.8^m$ ,  $\delta = -1^\circ 57'$ ).

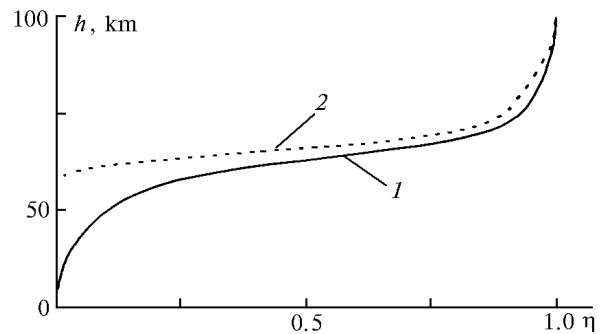


FIG. 1. Altitude dependence of brightness attenuation for the star No. 252 (Ref. 10) at its set behind the Earth's atmosphere: with regard for sensitivity of a specific photoreceiving device (1); for monochromatic radiation at  $\lambda = 255$  nm (2).

Spectral dependence of power illumination produced by the star is shown in Fig. 2. When calculating the curve 1, we used the experimental curve of spectral sensitivity of the specific photoreceiving device, which parameters allow its use in flight tests of equipment. For comparison, Fig. 1 presents the calculated altitude dependence (curve 2) of signal attenuation for a star when measuring in monochromatic light at  $\lambda = 255$  nm.

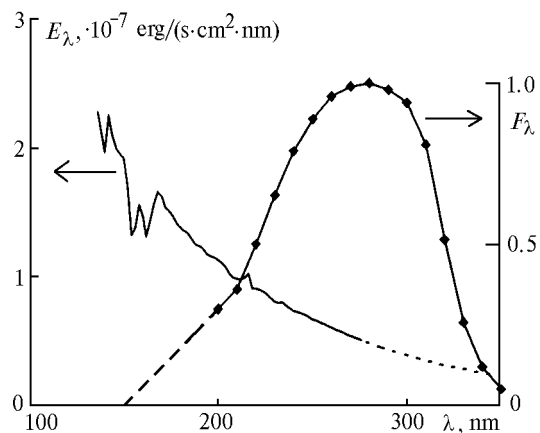


FIG. 2. Spectral dependence of power illumination  $E_\lambda$  produced by the star No. 252 (Ref. 10).  $F_\lambda$  is the relative spectral sensitivity of the specific photoreceiving device.

Onboard software for providing for the independent navigation contains two main algorithms for determining the height of star line of sight. The first algorithm serves for height computation from the forecasted position of a satellite determined with regard for values of all geopotential perturbations with the required accuracy. This algorithm is exact numerical algorithm. The second algorithm computes the height from the observation data on star brightness attenuation from a satellite. In the case, when curves of star brightness attenuation calculated at this stage based on the available atmospheric models have a systematic error, systematic errors in height estimation of the line of sight arise for all observed stars, i.e. the measurement errors correlate with each other. As known,<sup>11</sup> in independent navigation based on measurement of star heights above the horizon, if errors of height estimation are independent and distributed by the normal law with zero mathematical expectation, then operation of the navigation filter is characterized by the fact that rms errors in determination of orbit elements are proportional to the error of single measurements of a height and inversely proportional to  $\sqrt{N}$ , where  $N$  is the number of star observations. If errors of star height measurements correlate with each other, then, in the worst case, accuracy of determination of navigation parameters does not become better with the increasing number of reference star observations.

To work out the technical and methodical aspects of the considered method for determination of spacecraft navigation parameters, the special experimental equipment and the program were elaborated for performing experiments from onboard a geostationary satellite.

From the methodical point of view, the experiments are aimed at refinement of the average altitude behavior of the star brightness attenuation curves in comparison with the model curves, experimental estimation of the value of their variations, elaboration of algorithms for determination of spacecraft navigation parameters, and experimental estimation of the total error of this technique.

In the future, at the next stage of development, we plan to create the system allowing the simultaneous solution, in the independent mode, of both the problem of spacecraft navigation and the problem of high-frequency orientation of a spacecraft with respect to stars. The system is characterized by small size, weight, and energy consumption, as well as high accuracy. It is the system of celestial field sensors operating in the UV and visible ranges under control of a special video processor.

Figure 3 presents the scheme of wide-angle optical star sensor for independent navigation and orientation of a spacecraft. In accordance with calculation data, sensor of the Cassegronian meniscus system possesses high image quality (for the field  $2\omega \sim 7^\circ$ , spot size of a point source image does not exceed  $10 \mu\text{m}$ ). The sensor can work with any photoreceiving device, it possesses a

plane field of view, and its production is technological (all surfaces are spherical). Meniscus is made of melted quartz with pass band up to 200 nm. The objective diameter is  $D = 42.5 \text{ mm}$ , the equivalent focus length is  $F = 164.5 \text{ mm}$ , light intensity is  $A = 3.87$ . The proposed size of the matrix photoreceiving device (MPhRD) is  $1000 \times 1000$  pixels.

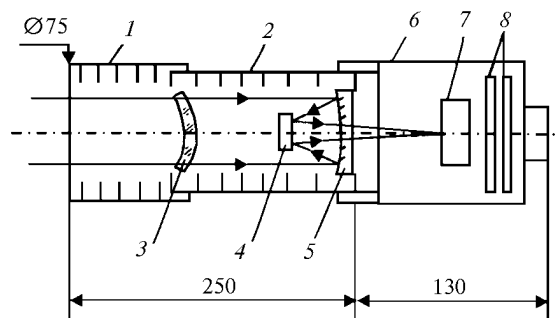


FIG. 3. Optical scheme of the wide-angle sensor: shade with a system of diaphragms (1); Cassegronian meniscus telescope (2); meniscus (3); secondary mirror (4); primary mirror (5); unit of the photoreceiving device (6); matrix photoreceiving device (7); control board of the matrix photoreceiving device (8).

Photosensitive CCD matrix with the number of elements  $2048 \times 2048$  was developed abroad for the problems of astronomy.<sup>12</sup> For more confident determination of star brightness, star images are suggested to be defocused.<sup>13</sup> According to calculations, spots  $60\text{--}80 \mu\text{m}$  in size (3–4 pixels of MPhRD) have angular size about 2 minutes of arc. At the supposed SNR, the methods of mathematical processing allow determination of the position of image center for stars of the 4th stellar magnitude accurate to a fraction of a pixel ( $\sim 0.15$  pixel). Accuracy of angle determination can increase by an order of magnitude in this case. The sensor can operate in both UV and visible spectral ranges. MPhRD in this case must be sensitive to UV radiation and equipped with special light filters providing for powerful suppression of visible radiation. Shade construction allows star observation at the distance more than  $30^\circ$  from the Sun. Sensor weight is about 2 kg, power consumption is 3 W.

Figure 4 shows composition and configuration of the system for independent navigation and high-accuracy navigation of a spacecraft. As seen from Fig. 4, the system includes two  $7^\circ$  UV sensors directed at the equator region and intended to perform the function of navigation parameters determination from the measurement data on star brightness attenuation at star set behind the Earth's atmosphere. They also can perform the function of orientation based on a celestial sky frame. Use of two UV sensors directed at the Earth's edge is the system guaranty in addition to the possibility of star attenuation observation during most of a day. Failure of one sensor decreases the resulting accuracy (time) of navigation parameters determination within allowable limits. The sensors 3 and 4 are

designed for spacecraft orientation with reference to stars. Use of a sensor directed at the Pole star allows high-accuracy determination of spacecraft orientation parameters continuously 24 hours a day, because the group of sensors 1, 2, and sensor 4 are directed approximately normal to each other and cannot be dazzled by the Sun at the same time. The fact that the sensors are oriented in the directions of three normal axes is system guaranty when solving the orientation problems. Failure of a sensor in one direction does not make impossible determination of spacecraft orientation parameters. In addition, any of the four sensors allow three-axes spacecraft orientation based on a celestial sky frame but with somewhat lower accuracy.

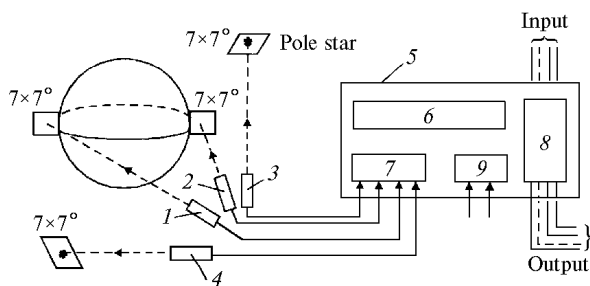


FIG. 4. Block diagram for spacecraft independent navigation and orientation: star field sensors (1 – 4): UV sensors directed to the equator region (1, 2), sensor (UV or visible) directed at the Pole star (3), sensor (UV or visible) with axis parallel to the spacecraft velocity vector (4); electronic unit (5): video processor (6), unit for control over sensors (7), unit for mating with onboard telemetric system of a spacecraft (8); power supply unit (9).

The structure of the electronic unit provides for a single functional solution to the problems of navigation and orientation. Every sensor is equipped with the control scheme (video signal generation) from matrices of PhRD sensor of  $1000 \times 1000$  (elements). All sensors are connected with the same electronic unit separately arranged onboard a spacecraft. This electronic unit comprises of the special processor for video information processing (either Russian video processor of 1815 type or preferentially Texas Instruments processor), as well as the processor (1806 type) for control over the equipment and connection with onboard computer and other systems. The main functions of the special video processor are determined by the processing structure of a celestial sky frame.

Processing of a frame includes: equalizing, i.e. referring of signal intensity values for image elements to one average value of sensitivity; filtration and optimal linear detection of 2D pulses of star images; correction, i.e. compensation for image distortions caused by field aberrations, first of all, lens distortion and coma; recognition. The recognition procedure

includes separation of a brightest star on a frame; calculation of the vector of attributes that is central distances (distances between the reference star on a frame and other less bright stars taken in the order of decreasing brightness); identification that is searching for such area of the celestial sky among reference areas that most closely coincides with the initial area. Position of the recognized area of the celestial sky as compared to the reference one serves as a basis for determination of spacecraft orientation parameters (pitch, yaw, bank) and identification of reference stars.

As follows from the results of statistical experiments we conducted, the central distances as a vector of indications for identification of a celestial sky area by the set of characteristics – simultaneous resistance to average and maximum errors of determination of star center coordinates – are highly competitive with such indications as angular distances between stars.<sup>13</sup> However, the central distances are also more resistant to inaccuracy of brightness determination and to the presence of excess stars in a frame or loss of real stars. This factor is important, because many navigation stars are varying and falling of space debris particles within a frame is also possible.<sup>14</sup> The computations were performed based on the data from the Smithsonian Astrophysical Observatory Star Catalog.<sup>15</sup>

Thus, the system of celestial field sensors operating in the UV and visible spectral ranges under control of the special video processor can solve simultaneously the problems of independent navigation and orientation of a spacecraft. The system has relatively small size, mass, and energy consumption.

## REFERENCES

1. M.A. Chory., D.P. Hoffman., C.S. Major, and V.A. Spektor, AIAA Pap., No. 1826 (1984).
2. R. Goundley, R. White, and E. Gai, Journal of Guidance, Control and Dynamics 7, No. 2 (1984).
3. G.M. Krekov and S.G. Zvenigorodskii, *Optical Model of the Middle Atmosphere* (Nauka, Novosibirsk, 1990), 278 pp.
4. A.P. Aleksandrov, G.M. Grechko, A.S. Gurvich, et al., Fiz. Atmos. Okeana 26, No. 1, 5–16 (1990).
5. L.V. Granitskii, A.A. Cheremisin, V.A. Bartenev, and A.M. Il'inykh, Atmos. Oceanic Opt., in press.
6. G.M. Keating, D.T. Young, and M.C. Pitts, Adv. Space Res. 7, No. 10, (10)105–(10)115 (1987).
7. A.A. Ramazov and Yu.G. Sikharulidze, "Global Model of Density Variations of the Earth's Atmosphere, B" Preprint No. 73, Institute of Applied Mathematics, Moscow (1979), 30 pp.
8. J.R. Herman, J. Geophys. Res. 84, No. 7, 3701–3710 (1979).
9. A.L. Ostrovskii., B.M. Dzhuman, F.D. Zabolotskii, and N.I. Kravtsov, *Regard for Atmospheric Influence on Astronomic Geodesic Measurements* (Nedra, Moscow, 1990), 235 pp.

10. *Ultraviolet Bright-Star Spectrometric Catalogue*, European Space Agency, 8-10, rue Mario-Niris, 75 738, Paris Cedex 15. France.
11. V.V. Ivashkin, *Kosm. Issled.* **23**, No. 6, 803-813 (1985).
12. G. Woker, *Astronomic Observations* [Russian Translation] (Mir, Moscow, 1990), 352 pp.
13. G.A. Avanesov, E.P. Aleksashin, G.A. Aleksashina, et al., in: *Optoelectronic Devices in Space Experiments* (Nauka, Moscow, 1983), pp. 124-157.
14. V.L. Ivanov, V.A. Men'shikov, L.A. Pchelintsev, and V.V. Lebedev, *Space Debris*, (Patriot, Moscow, 1996), Vol. 1, 360 pp.
15. N.G. Roman and W.H. Warren, Sr. *Smithsonian Astrophysical Observatory Star Catalog*, Version 1984, NSSOC/WDC-A-R&S. 84-02, January 1984.